CODEN IEJMAT *Internet Electronic Journal of Molecular Design* **2006**, *5*, 89–101 ISSN 1538–6414
BioChem Press http://www.biochempress.com

Inter*net* Electronic Journal of Molecular Design

February 2006, Volume 5, Number 2, Pages 89–101

Editor: Ovidiu Ivanciuc

Special issue dedicated to Professor Danail Bonchev on the occasion of the 65th birthday

Structural and Spectroscopic Studies of Chlorophyll c3 using DFT and TD–DFT Methods

Mama Nsangou,[1] Nejm–Eddine Jaïdane,[2] and Zohra Ben Lakhdar [2]

[1] Faculté des Sciences, Université de Ngaoundéré, B.P. 454 Ngaoundéré, Cameroun
[2] Laboratoire LSAMA, Faculté des Sciences de Tunis, Université Tunis El Manar, Campus Universitaire 1060, Tunis, Tunisie

Received: December 29, 2005; Revised: February 7, 2006; Accepted: February 14, 2006; Published: February 28, 2006

Citation of the article:
M. Nsangou, N.–E. Jaïdane, and Z. B. Lakhdar, Structural and Spectroscopic Studies of Chlorophyll c3 using DFT and TD–DFT Methods, *Internet Electron. J. Mol. Des.* **2006**, *5*, 89–101, http://www.biochempress.com.

Inter*net* Electronic Journal of Molecular Design

BioChem Press
http://www.biochempress.com

Structural and Spectroscopic Studies of Chlorophyll c3 using DFT and TD–DFT Methods

Mama Nsangou,[1,*] Nejm–Eddine Jaïdane,[2] and Zohra Ben Lakhdar [2]

[1] Faculté des Sciences, Université de Ngaoundéré, B.P. 454 Ngaoundéré, Cameroun
[2] Laboratoire LSAMA, Faculté des Sciences de Tunis, Université Tunis El Manar, Campus Universitaire 1060, Tunis, Tunisie

Received: December 29, 2005; Revised: February 7, 2006; Accepted: February 14, 2006; Published: February 28, 2006

Internet Electron. J. Mol. Des. **2006**, *5* (2), 89–101

Abstract

Motivation. In the present paper we use quantum chemical methods to optimize the molecular structure of the chlorophyll c3 (*Chl.c3*) and determine its molecular parameters and charges. Two theoretical methods have been used in this study, namely modified neglect of differential overlap with *d*–orbitals on some atoms (MNDO–d) and the density functional theory (DFT). In the DFT calculations we have used the Becke three parameters (B3) exchange functional, combined with the Lee–Yang–Parr (LYP) correlation functional. The time dependent density functional theory (TD–DFT) was used In the calculation of excited states.

Method. The molecular structure of the *Chl.c3* and the *Chl.c3* dimer has been successfully optimized and shows that the *chl.c3* macrocycle is non planar. In the monomer the Mg atom, coordinated to four nitrogen atoms, is neither located at the center nor in the porphyrin plane. Furthermore, TD–DFT calculations have successfully predicted the UV/visible absorption spectra of the *Chl.c3*.

Conclusions. The molecular structure and spectra predicted may help in an extensive experimental study of the ground– and excited–states of the *Chl.c3* molecular system.

Keywords. Chlorophyll c3; PM3; MNDO–d; DFT; B3LYP; 6–31G*; HOMO; LUMO.

Abbreviations and notations

PM3, Parameter Model three	B3LYP, Becke three–Lee–Yang–Parr
TD–DFT, Time Dependent – Density Functional Theory	*Chl.c3*, Chlorophyll c3
MNDO, Modified Neglect of Differential Overlap	AM1, Austin Model 1
ZINDO, Zero Intermediate Neglect of Differential overlap	CNDO, Complete Neglect of Differential Overlap
PM5, Parameter Model five	CI, Configuration Interaction
HOMO, Highest Occupied Molecular Orbital	LUMO, Lowest Unoccupied Molecular Orbital

1 INTRODUCTION

Chlorophylls (a, b, c1, c2, c3, d), Mg–chlorin, Mg–porphin, bacteriochlorin, bacteriochlorophylls and pheophytins are of central importance in many biological processes and biochemical reactions such as oxygen transport and storage, light absorption and electron transfer [1,2]. Because of this

Dedicated on the occasion of the 65th birthday to Danail Bonchev.

* Correspondence author; phone: 00–237–764–52–10; E–mail: mnsangou@yahoo.com.

importance these molecular systems have been subject of many theoretical and experimental investigations. In particular, the molecular structures [3–25] and the electronic structures [26–39] of the ground– and excited–states of these molecular systems have been widely studied.

Semi empirical methods (AM1, PM3, MNDO, PM5, MNDO–d, CNDO/S, ZINDO/S) were the first choice for estimation of the molecular structures and spectroscopic transition energies of photosynthetic chromophores listed above. However, the drawback is that under the harsh approximations of the semi empirical methods, they sometimes fail in the description of the properties to be estimated.

Linnanto and Korppi–Tommola [20,21] clearly pointed out that the PM3 method fails in the prediction of coordinates and atomic charges of magnesium and nitrogen atoms (particularly in the case of the chlorophyll c3, *Chl.c3*). It also turned out from their calculations that PM3–CI methods do not predict oscillator strengths very well and they concluded that the failure of the PM3 method was a reflection of its inadequate parameterization. In the present paper we use quantum chemical MNDO–d [40–42] and DFT [42–45] methods to optimize the molecular structure of the *Chl.c3* and determine its molecular parameters and charges. Since time–dependent density functional theory (TD–DFT) has been established as an extensive, efficient and reliable technique for studying electron correlations in the excited states of many molecules and molecular systems including porphyrins [37–39], this method is used for the calculations of electronic excited states parameters (wavelengths, oscillator strengths and excitation energies) of the *Chl.c3*.

2 COMPUTATIONAL METHODS

Calculations of the equilibrium structure and vibrational force field of the *Chl.c3* molecule was performed. The MNDO–d semi empirical method implemented in the molecular packing program MOPAC 2000 [41] was first used to derive the initial structure of the *Chl.c3* monomer that was then used for the following DFT calculations. It is important to mention that the MNDO–d method considers only valence *s*–, *p*– and *d*–functions, which are taken as Slater Type Orbitals (STO) with corresponding exponents ζ_s, ζ_p and ζ_d [40,41]. Further, this method uses restricted basis set of one *s*–orbital, three *p*–orbitals and five *d*–orbitals per atom. The resulting geometry of the *Chl.c3* monomer was reoptimized at the non–local density functional level of theory. In the density functional theory (DFT), electron correlation is introduced through the Kohn and Sham method [42,43] based on the combinations of some density functional (exchange, correlation). In the present work, the hybrid functional Becke's three parameters (B3) [44] combined with the gradient corrected correlation functional of Lee–Yang–Parr [45] also denoted B3LYP is used.

The near ultraviolet (UV) and visible part of the electronic absorption spectra, excitation energies and oscillator strengths have then been calculated at the DFT level using the time–

dependent perturbation approach (TD–DFT) [46], based on the Runge–Gross theorem [47] and related to the linear response Hartree–Fock or random phase approximation method [48]. Throughout the DFT calculations (geometry optimization and vertical excitation), the split valence double zeta basis sets of Petersson and coworkers (6–31G*) [49] with *d*–polarization functions on heavy atoms have been used. In the optimizations, all intramolecular degrees of freedom were optimized with no symmetry constraints and converged until the largest component of nuclear gradient was 10^{-6} a.u/bohr and the change in total energy was less than 10^{-7} a.u. The calculated vibrational frequencies at the equilibrium geometry gave real values, meaning that the geometry is a local or global minimum on the potential energy surface. In order to calculate the natural charges and describe the MgN bonding in terms of natural hybrid orbitals, we have used the natural bond orbital (NBO) procedure [50], implemented in the Gaussian03W computational package [51]. All the calculations have been performed on the MOPAC2000 [41] and Gaussian03W [51] computational packages.

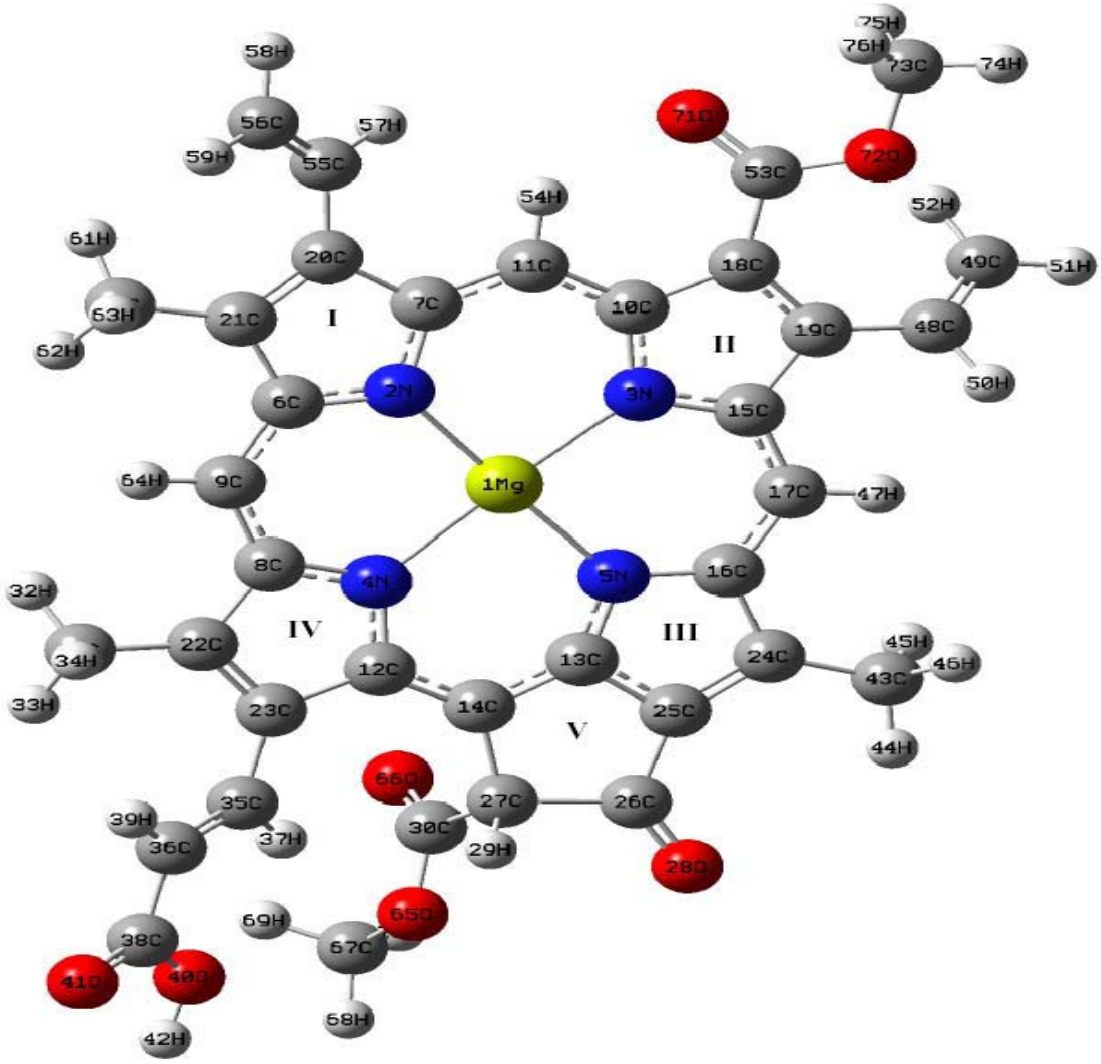

Figure 1. Equilibrium geometry of chlorophyll c3 as derived from DFT/B3LYP (6–31G*) calculations.

3 RESULTS AND DISCUSSION

3.1 Structure

3.1.1 The magnesium atom

The DFT optimized geometry of the *Chl.c3* is shown in Figure 1. Some selected intramolecular bond lengths; bond angles and dihedrals of the above molecule are given in Table 1 in which they are compared with the PM3 results obtained by Linnanto and Korppi–Tommola [22] and with the X–ray experimental values published by Serlin *et al*. [19]. Before discussing these results, it is important to mention that there does not exist any X–ray crystal structure for *Chl.c3* molecule.

The X–ray crystal structure of ethyl chlorophyllide a dihydrate molecule, used as experimental reference, is the closest experimental structure available even though Mg atom is five–coordinate in this structure. Further, the PM3 results represent to our knowledge, the unique theoretical calculations undertaken on *Chl.c3*. At the DFT/B3LYP (6–31G*) level of theory, the MgN distances are calculated to be 2.028 Å, 2.089 Å, 2.106 Å and 2.018 Å respectively for MgN_2, MgN_3, MgN_4 and MgN_5. A more detailed analysis of these MgN distances shows that the MgN_4 bond is longer than the MgN distances towards the other three rings (I, II and III). Similar trends were observed, in the semi empirical MNDO–d structures of the *Chl.a* [23] and the *Chl.b* [24], as well as in the experimental X–ray structures of ethyl chlorophyllide a dihydrate [18] and ethyl chlorophyllide b dihydrate [19].

The corresponding bond angles (N–Mg–N) are calculated to be 176.7°, 178.2°, 91.0°, 92.0°, 87.3° and 89.7° respectively for N_3MgN_4, N_2MgN_5, N_2MgN_3, N_2MgN_4, N_3MgN_5 and N_4MgN_5. In the light of these values, it is noticeable that the Mg atom is neither located at the center nor in the porphyrin plane. The position of the Mg atom in the macrocycle of the *Chl.c3* is similar to that of the said atom in the macrocycles of the chlorophyll a and the chlorophyll b calculated in our previous work using MNDO–d semi empirical method [23,24].

In contrast, this position is completely different from that determined with the PM3 method. This technique predicts the MgN_2 and MgN3 to be too long (2.361 Å and 2.424 Å), and the MgN_4 and MgN_5 to be too short (1.814 Å and 1.829 Å), showing the complete failure of the said method in the description of the Mg atom's position. Further, the DFT method predict as MNDO–d method that in *Chl.c3* and other chlorophyll monomers, the magnesium atom is coordinated to four nitrogen atoms, which therefore, reduce the Lewis acid character of the magnesium atom. This result is not consistent with the PM3 results, that are shown in Ref. [20] (see Figure 2), and that predict the Mg atom to be coordinated only to two nitrogen atoms.

Table 1. Selected DFT optimized bond lengths, bond angles and dihedrals of the chlorophyll c3. The PM3 theoretical results of Linnanto and Korppi–Tommola [22] are given in the third column. In the fourth and the last columns are given the X–Ray experimental values of Serlin *et al*.

Bond lengths				Bond angles and dihedrals		
	B3LYP 6–31G*	PM3 Ref. [22]	Ref. [19]		B3LYP 6–31G*	Ref. [19]
Mg_1N_2	2.028	2.361	2.063	$N_3Mg_1N_2$	91.0	89.3
Mg_1N_3	2.089	2.424	2.094	$N_4Mg_1N_2$	92.0	88.6
Mg_1N_4	2.106	1.829	2.167	$N_5Mg_1N_2$	178.2	158.2
Mg_1N_5	2.017	1.814	2.021	$N_4Mg_1N_3$	176.7	
C_6N_2	1.370	1.352	1.377	$N_5Mg_1N_4$	89.7	
C_7N_2	1.369	1.435	1.384	$N_5Mg_1N_3$	87.3	
$C_{10}N_3$	1.365	1.370	1.361			
$C_{15}N_3$	1.374	1.418	1.388	$N_2C_7C_{20}C_{21}$	–0.3	
C_8N_4	1.370	1.415	1.348	$N_2C_6C_{21}C_{20}$	–0.4	
$C_{12}N_4$	1.380	1.395	1.387	$C_6C_{21}C_{20}C_7$	0.4	
$C_{13}N_5$	1.342	1.342	1.347	$N_3C_{10}C_{18}C_{19}$	0.8	
$C_{16}N_5$	1.384	1.436	1.402	$N_3C_{15}C_{19}C_{18}$	0.3	
C_9C_6	1.399	1.434	1.388	$C_{10}C_{18}C_{19}C_{15}$	–0.6	
C_9C_8	1.405	1.364	1.383	$N_5C_{16}C_{24}C_{25}$	0.3	
$C_{11}C_7$	1.396	1.359	1.369	$N_5C_{13}C_{25}C_{24}$	0.3	
$C_{11}C_{10}$	1.408	1.432	1.418	$C_{13}C_{25}C_{24}C_{16}$	0.0	
$C_{14}C_{12}$	1.402	1.375	1.364	$N_4C_8C_{22}C_{23}$	0.0	
$C_{14}C_{13}$	1.405	1.426	1.397	$N_4C_{12}C_{23}C_{22}$	1.7	
$C_{17}C_{15}$	1.404	1.408	1.377	$C_{12}C_{23}C_{22}C_8$	–1.0	
$C_{17}C_{16}$	1.399	1.382	1.414	$C_{13}C_{25}C_{26}O_{28}$	–178.0	
$C_{18}C_{10}$	1.456	1.449	1.464	$C_{14}C_{27}C_{26}O_{28}$	176.2	
$C_{18}C_{19}$	1.389	1.394	1.361	$C_{14}C_{27}C_{30}O_{66}$	29.3	
$C_{19}C_{15}$	1.457	1.443	1.463	$C_{26}C_{27}C_{30}O_{66}$	–85.7	
$C_{20}C_7$	1.464	1.477	1.476	$C_{18}C_{19}C_{48}C_{49}$	–38.1	
$C_{21}C_{20}$	1.381	1.375	1.346	$C_{15}C_{19}C_{48}C_{49}$	139.6	
$C_{21}C_6$	1.454	1.472	1.451	$C_7C_{20}C_{55}C_{56}$	–152.1	
$C_{22}C_8$	1.451	1.482	1.525	$C_{21}C_{20}C_{55}C_{56}$	30.0	
$C_{22}C_{23}$	1.385	1.372	1.555	$C_{10}C_{18}C_{53}O_{71}$	—25.6	
$C_{23}C_{12}$	1.464	1.495	1.524	$C_{10}C_{18}C_{53}O_{72}$	152.5	
$C_{24}C_{16}$	1.458	1.466	1.420	$C_{19}C_{18}C_{53}O_{72}$	–23.5	
$C_{24}C_{25}$	1.384	1.381	1.404	$C_{14}C_{27}C_{26}C_{25}$	–4.5	
$C_{25}C_{13}$	1.425	1.456	1.416	$C_{13}C_{25}C_{26}C_{27}$	2.7	
$C_{26}C_{25}$	1.460	–	1.430	$C_{25}C_{13}C_{14}C_{27}$	–3.2	
$C_{26}C_{27}$	1.593	–	1.568	$C_{71}C_{53}C_{18}C_{19}$	–158.4	
$C_{27}C_{14}$	1.529	–	1.534			

3.1.2 Atomic charges

The net charges of magnesium, nitrogen and oxygen atoms calculated using the natural bond orbital (NBO) analysis and the Mulliken population, implemented in the Gaussian 03W program Package are listed in Table 2. It has been mentioned above that in *Chl.c3* the magnesium atom is coordinated to four nitrogen atoms, which therefore, reduce the Lewis acid character of the magnesium atom. This view is consistent with the calculations of Zerner and Gouterman [27] on the positive charge of metals in metalloporphyrins. The charges of N_2, N_3, N_4, N_5, O_{28}, O_{66}, O_{71} and O_{72} predicted by both techniques are negative while the Mg atom charge is positive. Similar results were obtained in the case of chlorophyll a and chlorophyll b by Nsangou *et al*. [23,24] using the

MNDO–d method and by Linnanto and Korppi–Tommola [21] using the PM5, the HF/6–31G* and the DFT/B3LYP (6–31G*) methods.

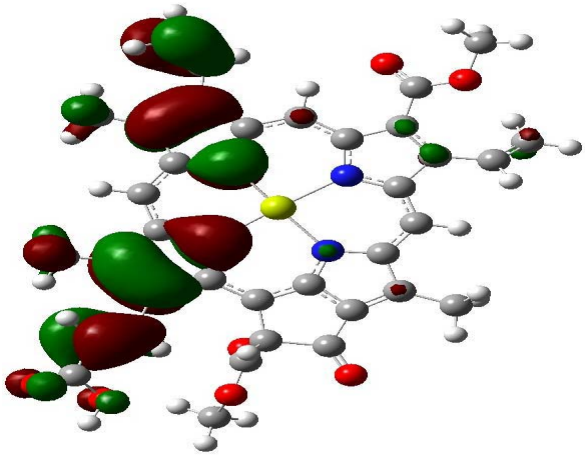

HOMO–2
(*a*)

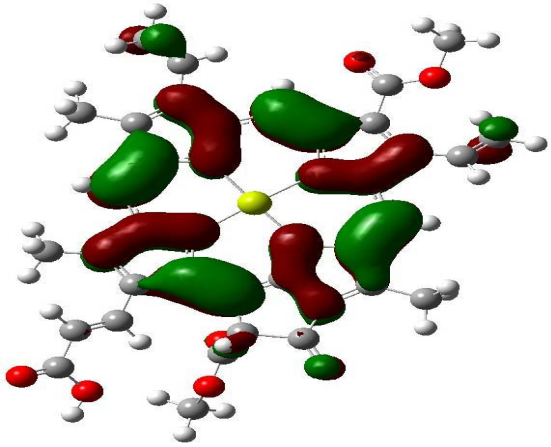

HOMO–1
(*b*)

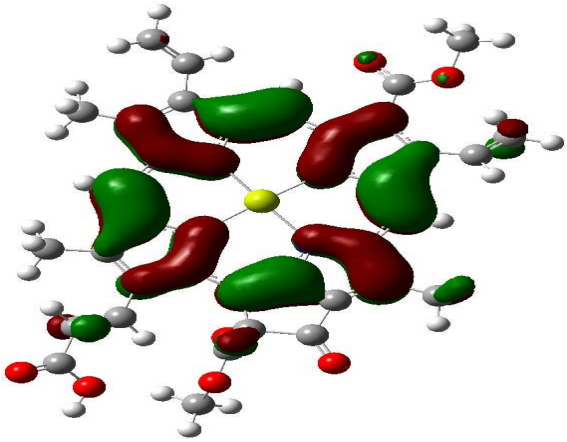

HOMO
(*c*)

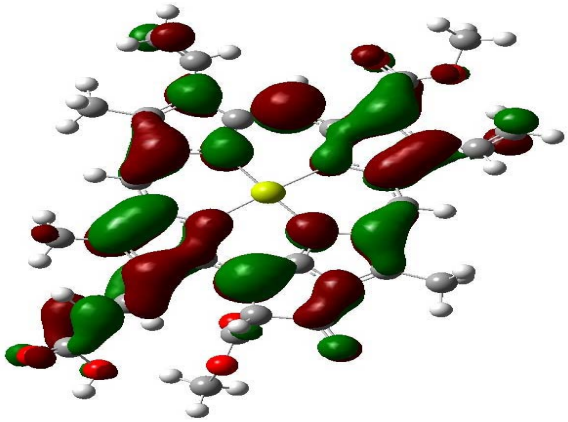

LUMO
(*d*)

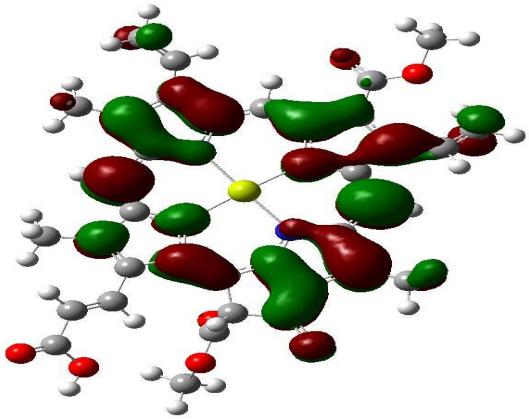

LUMO+1
(*e*)

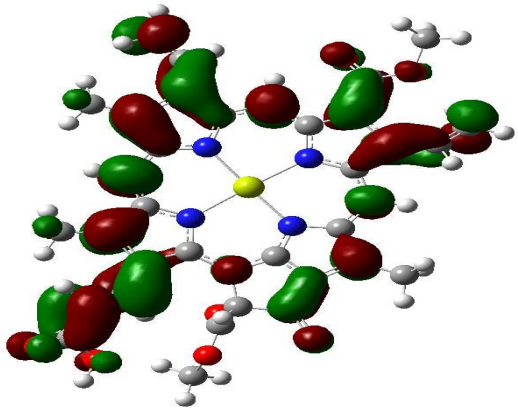

LUMO+2
(*f*)

Figure 2. Selected molecular orbitals contours of chlorophyll c3 from HOMO–2 to LUMO+2.

Table 2. Mulliken and NBO charges on some selected atoms

Atoms	Charges	
	NBO	Mulliken
Mg_1	1.703	0.869
N_2	–0.740	–0.751
N_3	–0.704	–0.731
N_4	–0.714	–0.733
N_5	–0.723	–0.762
O_{28}	–0.522	–0.457
O_{40}	–0.720	–0.584
O_{41}	–0.596	–0.484
O_{65}	–0.534	–0.438
O_{66}	–0.591	–0.470
O_{71}	–0.611	–0.500
O_{72}	–0.536	–0.451

Table 3. A part of calculated second order perturbation stabilization energies $E^{(2)}$ (kcal/mol) for donor–acceptor natural orbital interactions.

Donor NBO(*i*)	Acceptor NBO(*j*)	$E^{(2)}$ (*kcal/mol*)
LP(1)N(2)	LP*(1)Mg(1)	31.57
LP(1)N(3)	LP*(1)Mg(1)	27.68
LP(1)N(4)	LP*(1)Mg(1)	27.91
LP(1)N(5)	LP*(1)Mg(1)	30.20
BD(1)(N(2)–C(6))	LP*(1)Mg(1)	2.07
BD(1)(N(2)–C(7))	LP*(1)Mg(1)	2.12
BD(1)(N(3)–C(10))	LP*(1)Mg(1)	1.72
BD(1)(N(3)–C(15))	LP*(1)Mg(1)	1.72
BD(1)(N(4)–C(8))	LP*(1)Mg(1)	1.67
BD(1)(N(4)–C(12))	LP*(1)Mg(1)	1.52
BD(1)(N(5)–C(13))	LP*(1)Mg(1)	2.50
BD(1)(N(5)–C(16))	LP*(1)Mg(1)	1.96

In the NBO analysis, we focus on the stabilization energy $E^{(2)}$, calculated by the second order perturbation theory analysis of the Fock matrix [50]. Table 3 enumerates electron donor orbital *i*, electron acceptor orbital *j* and the stabilization energy $E^{(2)}$ between their interactions. It is well known that the larger the $E^{(2)}$ is, the stronger the interaction between them and the greater the tendency that *i* provide electron to *j*, *i.e.*, the more charges transferred [52]. It can be seen from Table 3, that the estimated values of $E^{(2)}$ between filed (donors) Lewis type NBOs (LP(1)N(2), LP(1)N(3), LP(1)N(4) and LP(1)N(5)) and empty (acceptor) non–Lewis NBOs (LP*(1)Mg(1)) are very large (31.57 kcal/mol, 27.68 kcal/mol, 27.91 kcal/mol and 30.20 kcal/mol) showing that electron density is significantly delocalized from the nitrogen atoms to the Mg atom. These values also show strong interaction between donors and acceptors NBOs and confirm the four coordination of the Mg atom mentioned above. In addition, the natural charges and Mulliken charges listed in Table 2 show that the Mg–N bonds are highly polarized, and are responsible of large shift of charge from magnesium to its neighbors. However, it is obvious from Table 2, that the Mulliken and NBO charges localized on the selected atoms are very different. This result is not surprising because the Mulliken scheme suffers from some approximations based on partitioning the wave function in terms of basis functions, and the fundamental problem is that basis functions often describe electron

density near a nucleus other than the one they are centered on. Consequently, atomic charges calculated from a Mulliken analysis will therefore not converge to a constant value as the size of the basis set is increased. In contrast, NBO's are linear combinations of the natural atomic orbitals and they form a localized picture of the atomic orbitals involved in the bondings. The further advantage of the natural atomic orbitals is that they are defined from the density matrix, guaranteeing that electron occupation is between 0 and 2, and that they converge to well–defined values as the size of the basis set is increased [42].

3.1.3 The macrocycle

Pyrrole rings are numbered clockwise (I, II, III and IV), and the cyclopentanone ring is numbered V as could be seen in Figure 1. Ring I is constituted of N_2, C_6, C_7, C_{20} and C_{21}, ring II is constituted of N_3, C_{10}, C_{15}, C_{18} and C_{19}, ring III is constituted of N_5, C_{13}, C_{16}, C_{24} and C_{25}, ring IV is constituted of N_4, C_8, C_{12}, C_{22} and C_{23}, ring V is constituted of C_{13}, C_{14}, C_{25}, C_{26} and C_{27}. The dihedrals characterizing each ring are listed in Table 1.

Their values show that except of ring IV and ring V in which the following dihedrals, $N_4C_{12}C_{23}C_{22}$ and $C_{12}C_{23}C_{22}C_8$, $C_{14}C_{27}C_{26}C_{25}$, $C_{13}C_{25}C_{26}C_{27}$, $C_{25}C_{13}C_{14}C_{27}$ are calculated to be respectively in absolute values 1.7°, 1.0°, 4.5°, 2.7° and 3.2°, others rings have their dihedrals less than 0.8°. This indicates that rings I, II and III may be considered as almost planar while rings IV and V are slightly distorted. The dihedrals $O_{28}C_{26}C_{27}C_{14}$, $O_{28}C_{26}C_{25}C_{13}$ for the keto oxygen O_{28}, and $O_{71}C_{53}C_{18}C_{10}$ and $O_{71}C_{53}C_{18}C_{19}$ for the carbomethoxy oxygen O_{71}, are calculated to be respectively 176.2°, 178.0°, 25.6° and 158.4°. These values clearly show that the keto oxygen O_{28} is displaced above the plane of ring V, while the carbomethoxy oxygen O_{71} is displaced below the plane of ring II. On the other hand there are two vinyl groups linked to the macrocycle at rings I and II as could be seen on Figure 1. The values of the dihedrals, $C_{56}C_{55}C_{20}C_7$, $C_{56}C_{55}C_{20}C_{21}$, $C_{18}C_{19}C_{48}C_{49}$ and $C_{15}C_{19}C_{48}C_{49}$ characterizing the displacements of both vinyl groups are calculated to be respectively 152.1°, 30.0°, 38.1°, 139.6°.

These values show that the vinyl group linked to ring I is 30.0° above the porphyrin plane while the second vinyl group linked to ring II is displaced by 39.0° below the said plane. It could also be observed in Figure 1 that the atoms of the interior ring of the homoporphyrin skeleton show a π–delocalization system, so that the displacements of C_{56} and C_{49} atoms respectively above and below the macrocycle reduce the extent of conjugation between the vinyl groups and the macrocyclic π–system.

Figure 2 shows that the four orbitals (from HOMO–1 to LUMO+1) of the chlorophyll c3 are well localized within the porphyrin ring. The HOMO–2 has higher amplitude on rings I and IV, the methyl and the vinyl groups linked to ring I, and on the methyl group linked to ring IV. In contrast, this orbital has very small or no amplitude on rings II, III and V, and groups linked to the said rings.

The LUMO+2 orbital has no amplitude on the carbomethoxy and the methyl groups linked to ring V, and no amplitude on the nitrogen atoms, but has large amplitudes on other rings and substituent groups of the molecule. The common feature of these molecular orbitals is that they have no amplitude on the Mg atom.

The *Chl.c3* dimer results from the self–assembly of two monomer subunits. Given its large size (152 atoms), its geometry is optimized with the MNDO–d semi empirical method. Figure 3 shows the optimized structure of the dimeric molecule. In this structure, the carbomethoxy carbonyl of one molecular subunit serves as an electron donor to relieve the coordination unsaturation of the central atom in its partner, and as an electron acceptor through the central atom to produce an array of pigment molecules linked together by C_{30} carbomethoxy C=O···Mg interactions. The overall dimeric molecule has a symmetrical behavior despite some discrepancies. The Mg–O bond lengths are calculated to be 2.12 Å. These observations are consistent with those of the chlorophyll a dimer [23] and the chlorophyll b dimer [24]. From Figure 3, one easily observes that the Mg atoms are neither located on the porphyrin macrocycles, and that the said macrocycles are nonplanar. Their distortions are due to the resulting strains applied on the acetyl oxygen O_{66} and its analog of the second subunit, and also the strong axial ligation (or direct covalent linkages) of the oxygen atoms of the carbomethoxy groups to the central Mg metals.

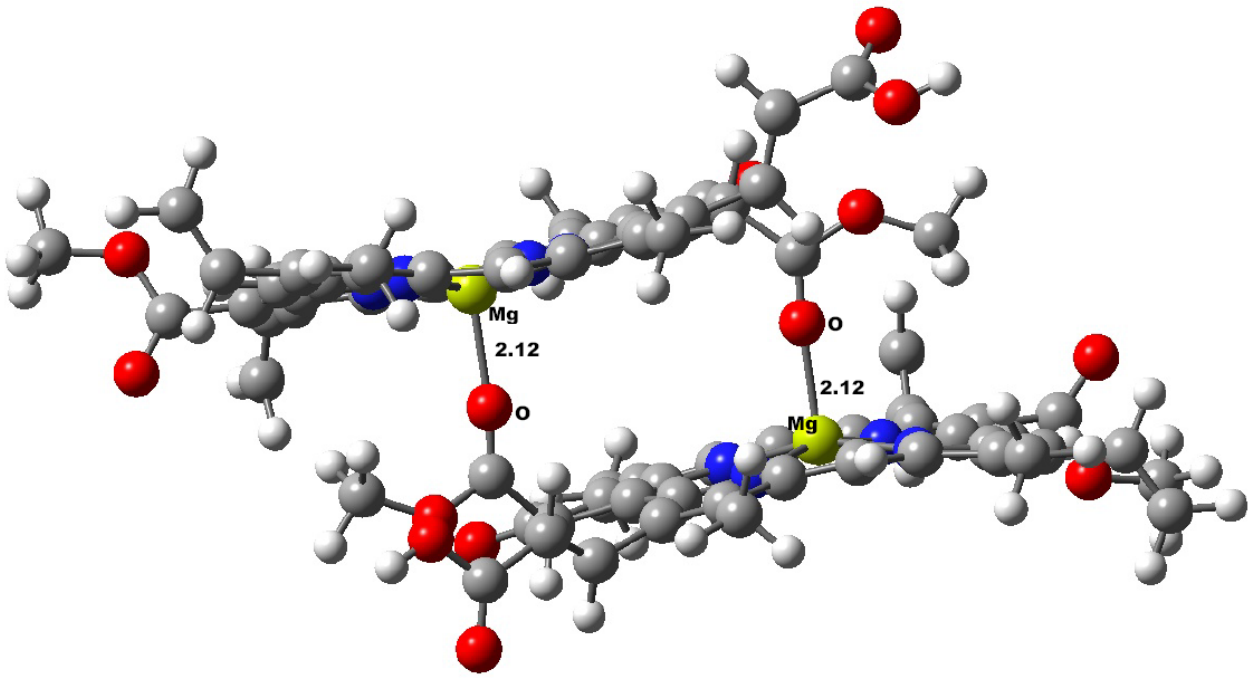

Figure 3. Equilibrium geometry of the Chlorophyll c3 dimer as derived from the MNDO–d semi empirical calculations.

3.2 Spectroscopy

In Table 4, the 8 lowest dipole–allowed singlet transitions energies (eV) and the corresponding wavelengths (*nm*) and oscillator strengths for *chl.c3* are compared with the available experimental and theoretical results. In gas phase, one absorption maximum is obtained in the Q band region at

625.34 *nm*, which corresponds to absorption energy of 1.98 eV. Comparing with other available results, one notices that the DFT/B3LYP calculated wavelength is in much closer agreement with the reported experimental value of 626 *nm* published by Jeffrey [54]. Other available theoretical results (PM5, CIS(5,5)/3–21G*, CIS(5,5)–ZINDO/S, PM3/CIS(5,5)) listed in Table 4 show clearly that TD–DFT>PM5> CIS(5,5)/3–21G*> CIS(5,5)–ZINDO/S> PM3/CIS(5,5). This comparison confirms that among the above–mentioned theoretical methods, DFT/B3LYP is the most accurate.

Table 4. Calculated excitation energies (*E*), transition wavelengths (λ) and oscillator strengths (*f*) for *Chl.c3* with the corresponding experimental and theoretical data. Coefficients in each configuration mixing are given in column three.

Excited states	Transitions	Coefficients	Excitation Energy (*E*)	λ (nm)	*f*
2^1A	164a→173a	0.11	1.9827	625.34	0.0744
	169a→171a	0.23		624.00[a]	0.08[a]
	169a→172a	–0.51		620.00[b]	0.10[b]
	170a→171a	0.68		609.00[c]	0.10[c]
	170a→172a	–0.26		593.00[d]	7.40[d]
				626.00[e]	–
3^1A	169a→171a	0.43	3.6232	342.19	1.8811
	170a→172a	0.36			
	170a→173a	–0.11			
4^1A	169a→172a	0.50	3.7731	328.60	1.5207
	170a→171a	–0.27			
5^1A	167a→171a	0.53	4.3338	286.09	0.1390
	167a→173a	0.22			
	168a→171a	0.26			
6^1A	167a→171a	0.20	4.3860	282.68	0.1921
	168a→171a	–0.35			
	168a→172a	0.42			
	168a→173a	0.27			
7^1A	163a→171a	0.14	4.6426	267.06	0.0310
	164a→172a	0.14			
	170a→173a	0.59			
	170a→174a	0.16			
8^1A	162a→171a	–0.15	4.6938	264.15	0.0035
	162a→172a	0.27			
	162a→173a	–0.19			
	162a→174a	–0.27			
	162a→177a	–0.26			
	162a→178a	0.19			
	162a→183a	0.12			

[a] PM5 semi empirical method [20]
[b] CIS(5,5)/3–21G* [20]
[c] CIS(5,5)–ZINDO/S [20]
[d] PM3/CIS(5,5) [20]
[e] Experiment [54]

The excitation spectra reported in Table 4 show that the number of electronic excited states involved in the Q band is greater than four, leading to the conclusion that the Gouterman's four orbital model [25–27,29] is not adapted.

Among the six subsequent excited states calculated, the strongest transitions appear at 342.19 *nm* and 328.60 *nm* with respective excitation energies of 3.62 eV and 3.77 eV. The configurations of both states, 3^1A and 4^1A, consist respectively of 0.43 (HOMO–1 → LUMO) + 0.36 (HOMO → LUMO+1) – 0.11 (HOMO → LUMO+2) and 0.50 (HOMO–1 → LUMO+1) – 0.28 (HOMO → LUMO). One could notice from these configurations that the 3^1A and 4^1A excited states are mostly described by the coupling of the following excitations: HOMO–1 → LUMO, HOMO → LUMO+1, HOMO–1 → LUMO+1 and HOMO → LUMO. Furthermore, the molecular orbital shapes of the orbitals involved in the above–mentioned excitations are well localized in the porphyrin ring as could be seen in Figure 2, and this probably explains the higher strength obtained for both states. Moreover, these two strongest transitions are obtained in the same range and may result in an absorption maximum not reported experimentally (or experimentally underestimated).

4 CONCLUSIONS

The DFT/B3LYP(6–31G*) calculations have provided detailed structural data for the *Chl.c3*, in vacuum. Comparison with the available experimental and calculated bond lengths, bond angles and dihedrals indicates that the DFT/B3LYP(6–31G*) method gives the better correlation than the PM3 method. However, some discrepancies in the C(α)–C(β) and C(β)–C(β) bond lengths, which may be due to molecular packing are noted. The structural parameters characterizing the macrocycle indicate that, in vacuum, *Chl.c3* is similar to *Chl.a* and *Chl.b* molecules. The preferred geometry of the macrocycle is non planar, despite the conjugative interactions. The central magnesium atom exhibits four coordination with weak covalent bonds to the nitrogen atoms of the four–pyrrole bases (or five coordination in the dimer). The predicted absorption wavelength by TD–DFT calculations is in good accordance with that observed experimentally.

Acknowledgment

One of the authors (M.N.) is highly indebted to Prof. Zohra Ben Lakhdar for her scientific support and warm hospitality during his stay in Tunisia. He also thanks the Abdus Salam ICTP (Trieste, Italy), Office of External activities, for their financial support (Grant N° LIBS–OEA–NET 45). The authors also express their gratitude to the referees for fruitful remarks.

Supplementary Material

The entire Cartesian coordinate of the chlorophyll c3 and the chlorophyll c3 dimer studied here are available upon request.

5 REFERENCES

[1] W. D. Scheidt, C. A. Reed, *Chem. Rev.* **1981**, *81*, 543.
[2] M. E. Michel–Beyerle, *in Antennas and Reaction Centers of Photosynthetic Bacteria*; Springer–Verlag: Berlin **1985**.
[3] G. L. Closs, J. J. Katz, F. C. Pennington, M. R. Thomas and H. H. Strain, *J. Am. Chem. Soc.* **1963**, *85*, 3809.
[4] J. J. Katz, R. C. Dougherty and J. G. Boucher, *Infrared and Nuclear magnetic resonance spectroscopy of chlorophylls*, *in The Chlorophylls*, L.P. Vernon and Seely, (Eds.), Academic Press: New York **1966**, pp 185.

[5] J. J. Katz, H. H. Strain, D.L. Leusing and R.C. Dougherty, *J. Am. Chem. Soc.* **1968**, *90*, 784.
[6] J. J. Katz, G. L. Closs, F. C. Pennington, M.R. Thomas and H.H. Strain, *J. Am. Chem. Soc.* **1963**, *85*, 3801.
[7] H. Scheer and J. J. Katz, *Nuclear magnetic resonance spectroscopy of porphyrins and metalloporphyrins*, *in Porphyrins and Metalloporphyrins*, Edited by K.M. Smith (Ed.), Elsevier: New York, **1975**, 399.
[8] T. R. Janson and J. J. Katz, *NMR spectra of diamagnetic porphyrins*, *in The Porphyrins*, D. Dolphin (Ed.), Academic Press: New York, **1978**, chap. 1.
[9] R. A. Goodman, E. Oldfiel and A. Allerhand, *J. Am. Chem. Soc.* **1973**, 7553.
[10] H. J. Brockmann, *Stereochemistry and absolute configuration of chlorophylls and linear tetrapyrroles*, *in The Porphyrins*, D. Dolphin (Ed.), Academic Press: New York, **1978**, chap. 9.
[11] H. Wolf, and H. Scheer, *Stereochemistry and chiroptic properties of pheophorbides and related compounds*, Ann. N.Y. Acad. Sci. **1973**, 206, 549.
[12] P. H. Hynninen and G. Sievers, *Conformations of chlorophyll a and a' and their magnesium free derivatives as revealed by circular dichroïsm and proton magnetic resonance*, *Z. Naturforsch*, **1981**, *B*36, 1000.
[13] M. Tasumi and M. Fujiwara, *Advances in Spectroscopy*, **1986**, *14*, 407.
[14] A. Rosilio and J.P. Leicknam, *Méthodes physiques d'analyse*, **1970**, *6*, 137.
[15] H. Fischer and H. Orth, *Die Chemie des Pyrrols*, 2 (2nd half), Akademische Verlagsgesellschaft, Leipzig; reprinted in (1968) Johnson reprint, New York **1940**.
[16] M. S. Fischer, D. H. Zakin and M. Calvin, *J. Am. Chem. Soc.* **1972**, *94*, 3613.
[17] C. Kratky and J.D. Dunitz, *Acta. Cryst.* **1975**, *B31*, 1586.
[18] H. C. Chow, R. Serlin, C. E. Strouse, *J. Am. Chem. Soc.* **1975**, *97*, 7230.
[19] R. Serlin, H.–C. Chow and C. E. Strouse, J. Am. Chem. Soc. **1975**, *97*, 7237.
[20] J. Linnanto and J. Korppi–Tommola, *Phys. Chem. Chem. Phys.* **2000**, *2*, 4962.
[21] J. Linnanto and J. Korppi–Tommola, *J. Comput. Chem.* **2003**, *25*, 123.
[22] http://www.rsc.org/suppdata/cp/b0/b004998k/Electrsublinfo.doc
[23] M. Nsangou, A. Ben Fredj, N. Jaidane, M.G. Kwato Njock, Z. Ben Lakhdar, *J. Mol. Struct. THEOCHEM.* **2004**, *681*, 213.
[24] M. Nsangou, A. Ben Fredj, N. Jaidane, M.G. Kwato Njock, Z. Ben Lakhdar, *J. Mol. Struct. THEOCHEM.* **2005**, *726*, 245.
[25] M. Gouterman, *J. Mol. Spectrosc.* **1961**, *6*, 138.
[26] M. Gouterman, L. Stryer, *J. Chem. Phys.* **1962**, *37*, 2260.
[27] M. Zerner and M. Gouterman, *Theoret. Chim. Acta*, **1966**, *4*, 44.
[28] C. Weiss Jr., *J. Mol. Spectrosc.* **1972**, *44*, 37.
[29] M. Gouterman, *in the Porphyrin*, D. Dolphin (Ed.); Academic Press: New York, **1978**,Vol.III.
[30] R. E. Christoffersen, *Int. J. Quant. Chem.* **1979**, *16*, 573.
[31] U. Nagashima, T. Takada, K.J. Ohno, *J. Chem. Phys.* **1986**, *85*, 4524.
[32] M. A. Thomson, M.C. Zerner, *J. Am. Chem. Soc.* **1991**, *113*, 8210.
[33] P. O. J. Scherer, C. Scharnagel, S.F. Fisher, *Chem. Phys.* **1995**, *197*, 333.
[34] L.Y. Zhang, R.A. Friesner, *J. Phys. Chem.* **1995**, *99*, 16479.
[35] T. Sakuma, T. Kashiwagi, H. Takada, H. Nakamura, *Int. J. Quantum Chem.* **1997**, *61*, 137.
[36] J. Hasegawa, Y. Ozeki, K. Ohkawa, M. Hada, H. Nakasutji, *J. Phys. Chem.* **1998**, *B102*, 1320.
[37] D. Sundholm, *Chem. Phys. Lett.* **1999**, *302*, 480.
[38] D. Sundholm, *Chem. Phys. Lett.* **2000**, *317*, 392.
[39] D. Sundholm, *Chem. Phys. Lett.* **2000**, *317*, 545.
[40] W. Thiel and A. A. Voityuk, *Theor. Chim. Acta.* **1992**, *81*, 391.
[41] J. J. P. Stewart, *J. Computer–Aided Mol. Design*, **1990**, *4*, 101; J. J. P. Stewart, *MOPAC 2000 Reference Manual*, Fujitsu Limited, **1999**.
[42] F. Jensen, *Introduction to computational Chemistry*, John Wiley and Sons Ltd, **1999**.
[43] W. Kohn, L. J. Sham, *Phys. Rev.* **1965**, *140*, 1133.
[44] A. D. Becke, *Phys. Rev.* **1988**, *A38*, 3098.
[45] C. Lee, W. Yang, R.G. Parr, *Phys. Rev.* **1988**, *B37*, 785.
[46] R. Bauernschmitt, R. Ahlrichs, *Chem. Phys. Lett.* **1996**, *256*, 454; R. Bauernschmitt, M. Haser, O. Treutler, R. Ahlrichs, *Chem. Phys. Lett.* **1997**, *264*, 573; M. E. Casida, C. Jamorski, K. C. Casida, D. R. Salahub, *J. Chem. Phys.* **1998**, *108*, 4439.
[47] E. Runge, E. K. U Gross, *Phys. Rev. Lett.* **1984**, *52*, 997.
[48] J. Olsen P. Jorgensen, in D. R. Yarkony (Ed.), *Modern Electronic Structure Theory*, Vol. 1, World Scientific, **1995**.
[49] G. A. Petersson, M. A. Al–Laham, *J. Chem. Phys.* **1991**, *94*, 6081; G. A. Petersson, A. Bennet, I. G. Tensfeldt, W. A. Shirley, J. Mantzaris, *J. Chem. Phys.* **1988**, *89*, 2193.
[50] E. D. Glendening, A. E. Reed, J. E. Carpenter, F. Weinhold, NBO Version 3.1.; A. E. Reed, L. A. Curtiss, F.

Weinhold, *Chem*. *Rev*. **1988**, *88*, 899.
[51] Gaussian 03, Revision B.05, M.J. Frisch, G.W. Trucks, H.B. Schlegel, G.E. Scuseria, M.A. Robb, J.R. Cheeseman, J.A. Montgomery, Jr. T. Vreven, K.N. Kudin, J.C. Burant, J.M. Millam, S.S. Iyengar, J. Tomasi, V. Barone, B. Mennucci, M. Cossi, G. Scalmani, N. Rega, G.A. Petersson, H. Nakatsuji, M. Hada, M. Ehara, K. Toyota, R. Fukuda, J. Hasegawa, M. Ishida, T. Nakajima, Y. Honda, O. Kitao, H. Nakai, M. Klene, X. Li, J.E. Knox, H.P. Hratchian, J.B. Cross, C. Adamo, J. Jaramillo, R. Gomperts, R.E. Stratmann, O. Yazyev, A.J. Austin, R. Cammi, C. Pomelli, J.W. Ochterski, P.Y. Ayala, K. Morokuma, G. A. Voth, P. Salvador, J. J. Dannenberg, V.G. Zakrzewski, S. Dapprich, A.D. Daniels, M.C. Strain, O. Farkas, D. K. Malick, A. D. Rabuck, K. Raghavachari, J. B. Foresman, J.V. Ortiz, Q. Cui, A.G. Baboul, S. Clifford, J. Cioslowski, B.B. Stefanov, G. Liu, A. Liashenko, P. Piskorz, I. Komaromi, R.L. Martin, D.J. Fox, T. Keith, M.A. Al–Laham, C. Y. Peng, A. Nanayakkara, M. Challacombe, P.M.W. Gill, B. Johnson, W. Chen, M.W. Wong, C. Gonzalez, and J.A. Pople, *Gaussian Inc*., Pittsburgh PA, **2003**.
[52] J. F. Lin, C. C. Wu, M. H. Lien, *J. Phys*. *Chem*. **1995**, *99*, 16903.
[53] A. D. Trifunac, J. J. Katz, *J. Am*. *Chem*. *Soc*. **1974**, *96*, 5233.
[54] S. W. Jeffrey, *Biochim*. *Biophys*. *Acta*, **1966**, *177*, 456.

Biographies

Mama Nsangou is senior lecturer of molecular physics at the University of Ngaoundere (Cameroon). After obtaining a Ph.D. degree in physical science from the University of Yaounde I (Cameroon), Dr. Mama Nsangou undertook postdoctoral research with Professor Zohra Ben Lahkdar at the University of Tunis El Manar (Tunisia). More recently, Dr. Nsangou is collaborating with Professor Ghomi (Université Paris13, France) on the study of the interaction of cationic peptides with antisense oligonucleotides. Dr. Mama Nsangou is Regular Associate of the Abdus Salam International Center for Theoretical Physics (Trieste, Italy) and its research activity is focused on the structural study of chlorophylls, small negative molecules and of the interaction of cationic peptides with antisense oligonucleotides. M.N. is married and father of two children.

Nejm–Eddine Jaïdane is professor at the Department of Physics – Faculty of Science – University of Tunis El Manar (Tunis, Tunisia). Professor Nejm–Eddine Jaïdane is Head of the Department of Physics. Its research activity is focused on the molecular structure and spectroscopy of small and large molecules. He is married and father of two children.

Zohra Ben Lakhdar is professor at the Department of Physics, Head of the laboratory of Atomic Molecular Physics and Applications. In 2005, she has been awarded the world L'OREAL prize for Africa. Professor Zohra Ben Lakhdar is Senior Associate of the Abdus Salam International Center for Theoretical Physics (Trieste, Italy). She works on plasma physics, and molecular structure and spectroscopy of small and large molecules. Professor Zohra Ben Lakhdar is married and mother of two children.